Parameters of convective atmospheric boundary layer as estimated with the eddy resolving model and by acoustic sensing

V.A. Shlychkov[1] and S.L. Odintsov

Institute of Atmospheric Optics,
Siberian Branch of the Russian Academy of Sciences, Tomsk
[1] Novosibirsk Affiliate of the Institute of Water and Ecological Problems,
Siberian Branch of the Russian Academy of Sciences, Novosibirsk

Received April 16, 2001

Based on the numerical eddy resolving model, the structure of the atmospheric boundary layer in summer is studied with allowance for the diurnal behavior of the surface temperature. The model calculations are compared with the sodar data obtained at the Institute of Atmospheric Optics. It is shown that the model well represents convective processes, including the dynamics of the mixing layer thickness, amplitude of the vertical speed fluctuations, and the characteristic scales of atmospheric thermics.

In the morning hours, as the surface heats up, unstable stratification is formed in the atmospheric surface layer. This process is especially pronounced in summer at fine weather and low advection. As the surface temperature increases, the thermal energy is accumulated in the lower layers, thus leading to the increase in the thickness of the unstable layer. The instability energy releases in the form of penetrating convection. Rising thermics transfer heat to the upper, stably stratified layers, and compensating downward motions move the upper-lying cold air to the near-surface heated layer. Convection smoothes the vertical temperature difference and provides for formation of the mixing layer, whose thickness H_i increases, as the surface heats up, and can achieve 1000 m and more depending on the radiative balance, stratification of the free atmosphere, wind velocity, etc.

The equipment for acoustic sensing that arose in the last decade turned out to be efficient for identification of the parameters of the atmospheric boundary layer (ABL), as exemplified, in particular, in Refs. 1 and 2. Processing of the reflected sonic signal yields the position of the mixing layer top, and analysis of intensity variations of the echo signal gives an idea on the spatial scale of convective elements $ coherent structures.

Figure 1 shows the height-time scan of the envelope of signals recorded by the Volna-3 three-channel Doppler sodar developed and calibrated at the Institute of Atmospheric Optics.[3,4] The Volna-3 sodar is used to obtain the high-quality data on the intensity of temperature pulsations and the wind velocity. The presented results were obtained from the vertical sensing channel at the sensing pulse duration of 0.15 s and the period for estimation of one wind velocity profile equal to 15 s. The sodar was installed on a roof at the height of 12 m. In the facsimile record shown in Fig. 1, the degree of blackening reflects the mean value of temperature pulsations in the scattering volume.

Figure 1 demonstrates the cycle of destruction of the night (radiative) temperature inversion and the transition to the convective conditions. In the initial period, roughly till 09:30, all the ABL transformation processes occur inside the main turbulized layer 160$ 180 m thick (individual dark points and groups of points above 250 m correspond to external noise, such as birds, cars, etc. recorded by the sodar). Then the thickness of the layer with high reflectance that corresponds to the entrainment zone at the inversion boundary increases. As this takes place, convective processes associated with formation and rise of thermics (alternating sections with increased blackening) gradually develop under the inversion. The inversion was destroyed roughly by 12:00.

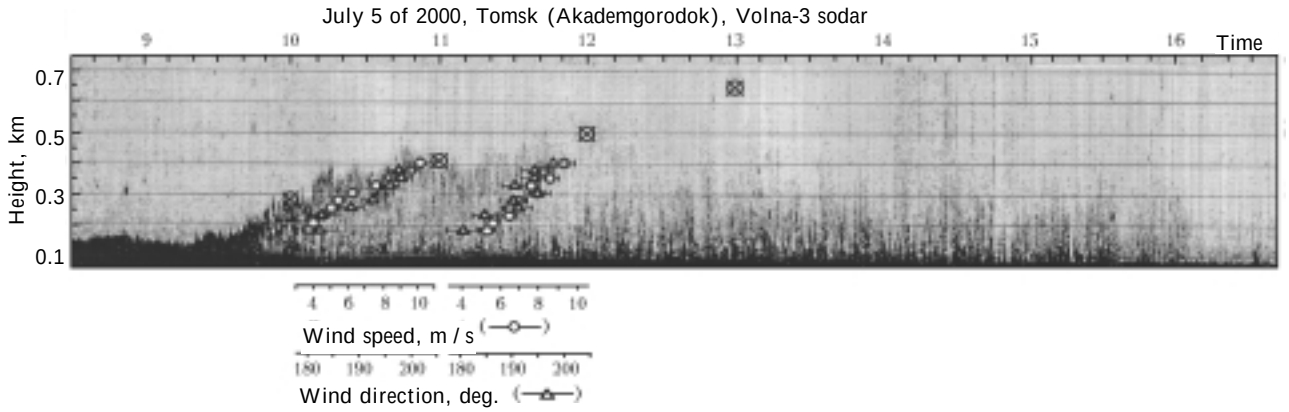

Fig. 1. Facsimile record of acoustic echo signal with two profiles of wind speed and direction averaged over the periods of 10:00$ 11:00 and 11:00$12:00. Circles with crosses mark the calculated boundary of the convective layer.

0235-6880 / 02 / 02 178-04 $02.00 I 2002 Institute of Atmospheric Optics

In accordance with the structure of the facsimile record, we can assume that the upper boundary of the temperature inversion at the time of its destruction was at the height of about 500$550 m. At this time, convection begins to dominate in the ABL. Some thermics reach the height $H_i \approx 600$ m, but more often they do not go higher than 400$450 m. Possibly, they reach higher heights, but temperature pulsations there are so small, that sodar already cannot distinguish them against the noisy background. The limit sensitivity of the Volna-3 sodar in the considered period with the use of the structure characteristic of temperature q_T^2 as a measure of intensity of temperature pulsations was about $5 \cdot 10^{\$7}$ K^2·m$^{\$2/3}$ (see Ref. 4). In the initial period (till 09:30), the value of q_T^2 achieved $10^{\$3}$ K^2·m$^{\$2/3}$ (for the heights of 100$180 m). Under the convective conditions, the intensity of temperature pulsations did not exceed $q_T^2 \approx 5 \cdot 10^{\$5}$ K^2·m$^{\$2/3}$. It should be noted that after 13:00 some clouds appeared and at the end of the measurement session they had the form of Cu, Cb with the cloud amount index of 6$8. Besides, after 14:00 the wind was gusty for about 45 min. This caused extra noise, which can be seen as solid vertical lines in the facsimile record (since 14:05 till 14:50).

The wind conditions for the period from 10:00 to 12:00 are shown in Fig. 1 by the speed (circles) and direction (triangles) plots with hour averaging (for 240 sensing cycles). Horizontal bars show the 90-% confidence intervals of these parameters.

It seems interesting to compare the measured value of H_i with the results of numerical simulation of the ABL in order to test the theoretical model against the observations. At the same time, the information obtained from simulation may prove useful for sodar adjustment and calibration.

To calculate the diurnal evolution of the convective ABL, we used the eddy resolving model[5] providing for the explicit description of coherent structures. The model is a numerical realization of nonstationary three-dimensional equations of fluid dynamics in the Boussinesq approximation. The vertical boundary conditions imply specification of the diurnal behavior of the surface temperature and decay of convective pulsations at the upper boundary lying at the level $z = 1500$ m. The horizontal dimensions of the area are $10 \cdot 10$ km^2, what allows structure elements of the stochastic ensemble with dimensions of 500 m and larger to be shown in detail on the 128×128 grid in the plane xy. Turbulent closing of sub-grid processes is based on the Smagorinsky equations and solution of evolutionary equations for the kinetic energy of turbulence and its dissipation rate.

The model of Ref. 5 is close to the LES (Large Eddy Simulation) models, which are now actively developed by foreign scientists.[6,7] In contrast to the œclassicalB numerical simulation, in the LES approach the spectrum of the resolved processes is extended due to the direct reconstruction of the ensemble of quasi-deterministic large eddies of turbulent origin. The basic assumption for construction of the models of turbulent penetrating convection is the double structure of the flow consisting of small-scale fluctuations with continuous energy spectrum (locally isotropic turbulence) and the set of self-organizing eddies.

Eddy resolving integration requires considerable computational resources. Thus, the typical time step in the LES models described in Ref. 6 is 1 s. In the model of Ref. 5, the time step was taken equal to 15 s. This is achieved due to the application of implicit finite-difference schemes based on the splitting method.[8] In addition, separate description of the mean fields in convective deviations in Ref. 5 allows radiative boundary conditions to be imposed on the large eddy components of the solution, which provide for the free exit from the area of fast gravitational waves. The above peculiarities make the model of Ref. 5 acceptable for computation on Pentium-3 PC.

According to the observations, the near-surface temperature varied from 18.7°C at 08:00 LT to 30.5°C at 17:00 LT, reaching the peak of 30.8°C at 15:00 LT. Taking into account the small spread in the wind direction (± 10°), let the axis . be oriented along the mean direction. The vertical profile of the geostrophic velocity U_G (as an analog of the baric gradient in the AB L) is specified as a step function, which is constant and equal to 3 m / s at $z < 100$ m, linearly increasing at $z \geq 100$ m with the gradient of 2.33 m / s / 100 m, and equal to 10 m / s above 400 m.

B ecause the data on the vertical temperature distribution were absent at the time of integration beginning (t_0 = 08:00 LT), the meteorological conditions on July 5 were thought typical of the summer season. The vertical profile of the potential temperature $\theta(z)$ is specified as a linear function of height with gradient $\theta_z = 8$°C / km in the lower 450-m layer and the standard value $\theta_z = 4$°C / km above $z = 450$ m. The accepted strongly stable stratification at the lower levels is an attempt to consider the night surface inversion.

These initial data were used in the calculation by the numerical model in order to describe the evolution of the convective AB L. The position of the model AB L height is marked by the crossed circles in Fig. 1. It can be seen that the calculated values of H_i are rather close to the actual position of the mixing layer top, at least, till 13:00. The following increase of the AB L thickness is connected with the continuing heat influx to the surface and the increase of its temperature till 15:00. The comparison of the actual and model values of H_i in this period may prove incorrect because of cloudiness and possible development of humid-convective processes, whose description is omitted in this consideration.

The evolution of H_i for the period of integration till 17:00 is shown as curve *5* (right scale) in Fig. 2. The thickness of the mixing layer increases monotonically with time and at 16:00 achieves the value of 1150 m, after that convective motions begin to gradually weaken.

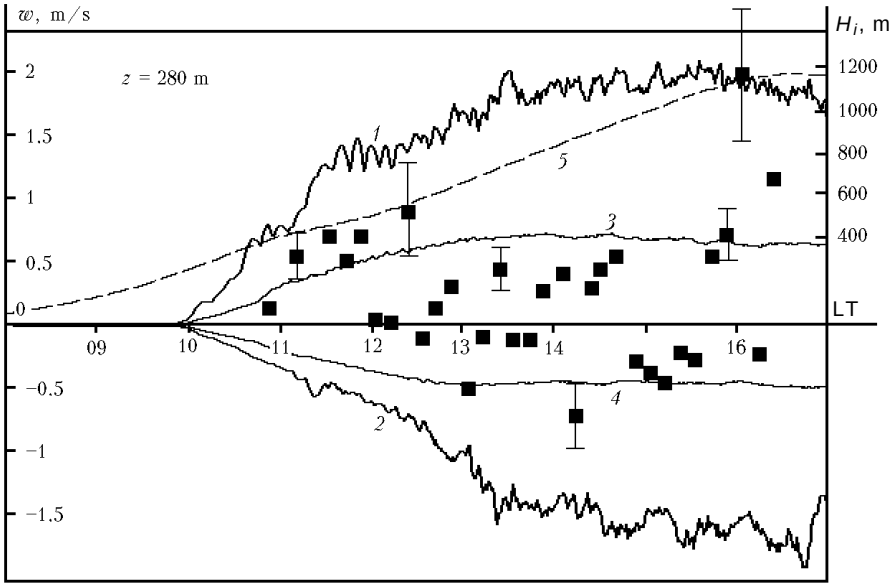

Fig. 2. Variation of extreme (curves *1*, *2*) and mean (curves *3*, *4*) upward and downward flows at the level z = 280 m: sensing data (closed squares), calculated top of the mixing layer (curve *5*) (right scale).

Curves *1* and *2* in Fig. 2 show the extreme values of the speed w of upward and downward flows at the level z = 280 m, and curves *3* and *4* show the horizontally mean values. Besides, Fig. 2 depicts the measured vertical speed (closed squares). Field measurements are given with 10-min averaging (six points an hour), and 90-% confidence intervals at some points are shown by vertical bars. Taking into account that the large eddy simulation can provide for obtaining correct statistical characteristics of a flow, although the detailed space and time pattern of such a pulsating motion does not reconstruct exactly some real process,[9] we come to the conclusion that the intensity of model convective motions well corresponds to the amplitudes of the measured vertical speed. The actual value of the pulsation speed lies nearby the mean values of w (curves *3* and *4* in Fig. 2), and at some time (about 16:00 LT, $w \approx 2$ m/s) achieves the extreme calculated values.

Figure 3 illustrates the horizontal structure of the field of w obtained from the model at t = 15:00 LT at the level z = 280 m (the isoline step is 0.5 m/s, gray color corresponds to the close-to-zero values of w). Figure 3 gives the general idea on the characteristic scales and configuration of convective elements in the horizontal plane.

Considering Fig. 1, notice the short-period formations in the convective layer, that distinguish by the intensity of blackening. If they are interpreted as structure elements of the convective ensemble, then their size can be estimated, knowing the mean speed of horizontal transfer with respect to a fixed observation site. According to numerical estimates, this speed is about 3\$4 m/s. Estimating visually the intervals of time inhomogeneities in Fig. 1 as 5\$10 min, we obtain that the actual dimensions of thermics in the direction of transfer are 900\$2400 m. Looking at the model field of w in Fig. 3 and separating visually individual formations, we can identify the size spectrum of convective elements as roughly 500\$3000 m, what corresponds to the observations.

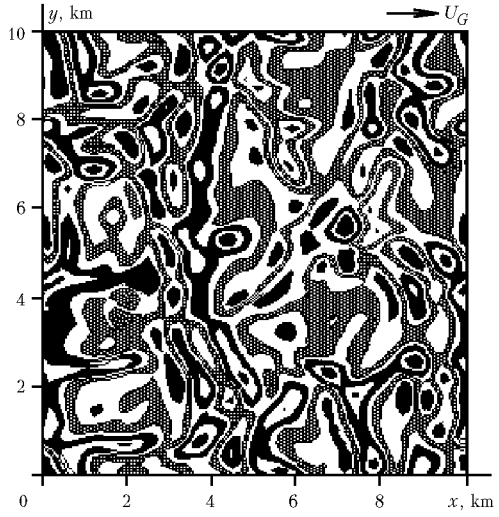

Fig. 3. Horizontal cross section of the field of w at z = 280 m, t = 15:00 with the step of 0.5 m/s.

To estimate the contribution of large eddy turbulence, the mean fields were calculated by the diffusion K-model neglecting convective exchange. This solution incorrectly reconstructs the vertical structure of the convective layer; in particular, the pronounced mixing layer is absent and the unstable stratification is not solved. This example demonstrates the importance of the mechanism of convective transfer in simulation of the diurnal ABL evolution.

Thus, the comparison of the results of sodar sensing and eddy resolving simulation has demonstrated the good agreement between the experimental data and numerical calculations. The mathematical model well reconstructs the structure of the convective ABL, including the mixing layer evolution (at least, in the initial 4-hour period of convection evolution). It can be concluded that the features of the inner structure of actual processes and the model convective ensemble are statistically close.

Acknowledgments

The authors are thankful to Professor P.Yu. Pushistov for useful criticism.

This work was partly (as applied to simulation of convective processes) supported by the Russian Foundation for Basic Research, Grant No. 99$05$64735.

References

1. M.A. Kallistratova, Int. J. Remote Sensing **22**, 251$266 (1994).
2. J. Kologiros, C. Helimis, and D. Asimakopulos, Boundary-Layer Meteorol. **91**, No. 3, 413$449 (1999).
3. V.A. Gladkikh, A.E. Makienko, and V.A. Fedorov, Atmos. Oceanic Opt. **12**, No. 5, 422$429 (1999).
4. V.A. Gladkikh and S.L. Odintsov, Atmos. Oceanic Opt. **14**, No. 12, 1050$1053 (2001).
5. V.A. Shlychkov, P.Yu. Pushistov, and V.M. Mal'bakhov, Atmos. Oceanic Opt. **14**, Nos. 6$7, 527$531 (2001).
6. F.T.M. Nieustadt, P.J. Mason, Ch.-H. Moeng, and U. Schumann, in: *Selected Papers from the 8th Symposium on Turbulent Shear Flow* (Springer-Verlag, New York, 1991), pp. 343$367.
7. B. Stevens and D.H. Lenschow, Bull. Amer. Meteorol. Soc. **82**, No. 2, 283$294 (2001).
8. G.I. Marchuk, *Methods of Computational Mathematics* (Nauka, Novosibirsk, 1973), 352 pp.
9. O.M. Belotserkovskii and A.M. Oparin, *Numerical Experiment as Applied to Turbulence: from Order to Chaos* (Nauka, Moscow, 2000), 223 pp.